A New Termination Condition for the Application of the TLM Method to Discontinuity Problems in Closed Homogeneous Waveguide

Luca Pierantoni, *Member, IEEE*, Cristiano Tomassoni, and Tullio Rozzi, *Fellow, IEEE*

***Abstract*—In this paper, we propose exact transmission-line matrix (TLM) boundary conditions for closed homogeneous waveguides. This approach is based on applying mode matching at the absorbing boundaries to the time-domain TLM algorithm. The absorbing condition in the time domain is achieved by the convolution of the modal characteristic impedances following inverse Fourier transform. The method is demonstrated for thick inductive irises in rectangular waveguide, showing excellent wide-band match of the fundamental mode, as well as of higher order modes excited by the discontinuity.**

***Index Terms*—Absorbing boundary conditions, modal analysis, time-domain analysis, transmission-line matrix (TLM) method, waveguide discontinuities.**

I. Introduction

THE application of space-discretizing methods such as the transmission-line matrix (TLM) [1] or finite-difference time-domain (FDTD) [2] often requires proper absorbing conditions at the limit of the computational domain. These conditions have to simulate either free-space or matched-load conditions in waveguide over a wide frequency band and for arbitrary wave incidence. In the past, many authors have proposed the absorbing-boundary condition (ABC) algorithm for TLM simulations, as in [3], where a Taylor series was used, or in [4], where a stability factor was introduced in order to prevent instabilities due to Higdon's conditions. In [5], super-absorbing conditions and the Johns matrix technique [6] were presented for waveguide problems. The perfectly matched layer (PML) technique originally proposed for FDTD field computations in open space [7] performs very well, but it requires the introduction and modeling of nonphysical materials, thus enlarging both the spatial domain and computational effort.

For the TLM method, the diakoptics procedure was introduced in [8] for the analysis of closed homogeneous waveguides. This technique is versatile and generates global absorbing boundaries, but requires the pre-computation and storage of the time-domain modal impulse response matrix of the semi-infinite waveguide [9]. In [10]–[13], a new termination condition for discontinuity problems in waveguide was introduced for the FDTD method. The above condition is based on the convolution proprieties of the modal characteristic impedance of the "accessible modes," i.e., the fundamental and first few below cutoff that possibly still cause interaction with adjacent discontinuities.

The goal of this paper is to derive exact (matched-load) modal absorbing boundary conditions (MABCs) in homogeneous waveguides for TLM applications by using analogous principles, as in [10], [11] for the FDTD method. The approach develops along the following lines.

- We chose reference planes where we intend to place the boundary conditions; on such planes, we interface the TLM discretized representation of the field with the modal one, analytical in the frequency domain.
- Incident TLM impulses upon the boundary are decomposed into modes, the modes are matched by using the inverse Fourier transform of the modal characteristic impedances, as in [10], and the reflected modes are recombined into TLM impulses, as in [9]. The effect of the above hybrid TLM–modal approach is to generate the exact boundary termination condition for any homogeneous waveguide structure once its frequency representation is known.

It is noted that, with respect to the diakoptic technique, we do not require any pre-computation and storage of the impulse response. In order to test the method, we analyze the classical problem of thick inductive irises in rectangular waveguide. We use the symmetrical condensed node (SCN) TLM [1]. Numerical results show very accurate wide-band match of the fundamental mode, as well as of the higher order modes excited by the discontinuity.

II. Theory

Referring to Fig. 1, let us suppose we want to place the matched load after the $(i_0 - 1)$th plane of the discretized space along the wave-propagation direction.

The basic idea is to consider the waveguide as infinitely long along the z-axis and to simulate analytically the behavior of the imaginary TLM nodes at the i_0th transverse plane. In practice, we do not need to evaluate the behavior of all TLM transmission lines of the imaginary nodes, but just the lines connecting these nodes to the nodes at the $(i_0 - 1)$th transverse plane. In other words, we require to evaluate the TLM reflected waves ${}_kb_{\mu,m,n}$ of the imaginary node lines from the incident TLM waves ${}_ka_{\mu,m,n}$, where k is the discrete time variable and m and n are the discrete transverse space coordinates, while μ represents the polarization and $\mathbf{r}$ represents the transverse position

Manuscript received May 13, 2001; revised January 8, 2002.

L. Pierantoni and T. Rozzi are with the Department of Electronics and Automatics, University of Ancona, 60100 Ancona, Italy (e-mail: l.pierantoni@ee.unian.it).

C. Tomassoni is with the Department of Electronic and Information Engineering, University of Perugia, 06100 Perugia, Italy.

Digital Object Identifier 10.1109/TMTT.2002.804622

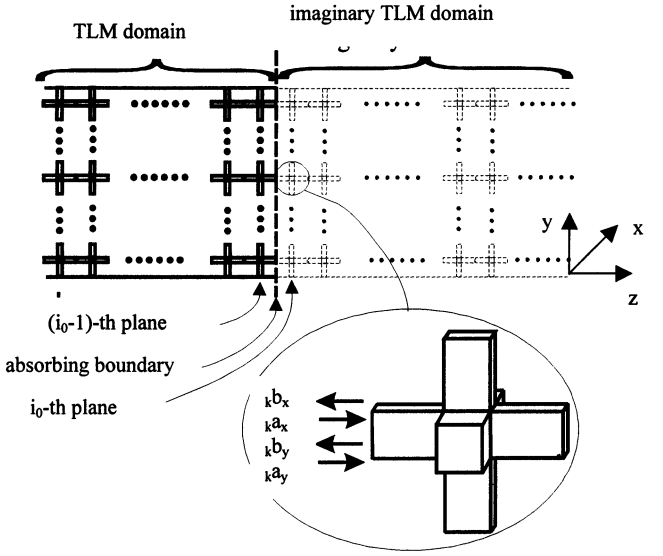

Fig. 1. Boundary interface between the TLM real nodes (at the (i_0-1)th transverse plane) and the TLM nodes of the extended imaginary waveguide (at the i_0th plane).

vector. In order to evaluate ${}_kb_{\mu,m,n}$, we express the transverse electromagnetic field by using both waveguide modes and TLM representation as follows:

$$\underline{\mathbf{E}}_t(\mathbf{r}) = \sum_n V_n(t)\underline{\mathbf{e}}_n(\mathbf{r}) = \sum_{k,\mu,m,n} ({}_ka_{\mu,m,n} + {}_kb_{\mu,m,n})T_k(t)\Phi_{\mu,m,n}(\mathbf{r})\underline{\mathbf{a}}_\mu \tag{1a}$$

$$\eta\underline{\mathbf{H}}_t(\mathbf{r},t) = \eta\sum_n I_n(t)\underline{\mathbf{a}}_z \times \underline{\mathbf{e}}_n(\mathbf{r}) = \underline{\mathbf{a}}_z \times \sum_{k,\mu,m,n} ({}_ka_{\mu,m,n} - {}_kb_{\mu,m,n}) \cdot T_k(t)\Phi_{\mu,m,n}(\mathbf{r})\underline{\mathbf{a}}_\mu \tag{1b}$$

where $\underline{\mathbf{a}}_\mu$ are the coordinate unit vectors, $\eta = (\mu_0/\varepsilon)^{1/2}$ is the free-space impedance, $\Phi_{\mu,m,n}(\mathbf{r})$ are the two-dimensional rectangular TLM spatial functions, and $T_k(t)$ is the TLM triangular time-domain function introduced in [1]. $V_n(t)$ and $I_n(t)$ are the modal expansion coefficients of the electric and magnetic field, respectively, and $\underline{\mathrm{e}}_n(\mathbf{r})$ are the modal electric-field eigenfunctions. Note that the modal magnetic-field eigenfunctions are written as $(\underline{\mathbf{a}}_z \times \underline{\mathbf{e}}_n)$, which is consistent with a TE/TM expansion of the field in the homogeneous guide.

For the sake of brevity, we consider in detail TE modes and just the final results for the TM case. By multiplying (1b) by $(-\underline{\mathbf{a}}_z)$, adding (1a) to (1b), and considering that the following relation holds [10]:

$$V_n(t) = Z_n(t) * I_n(t) = \eta\left[I_n(t) - \omega_n\int_0^t J_1(\omega_n\tau)I_n(t-\tau)\,d\tau\right] \tag{2}$$

where $Z_n(t)$ and ω_n are the wave impedance inverse transforms and the cutoff frequencies, respectively, of the nth mode, while $J_1(\omega_n\tau)$ is the Bessel function of the first kind and first order, we obtain

$$2\sum_{k,\mu,m,n} {}_ka_{\mu,m,n}T_k(t)\Phi_{\mu,m,n}(\mathbf{r})\underline{\mathbf{a}}_\mu = \eta\sum_n\left[2I_n(t) - \omega_n\int_0^t J_1(\omega_n\tau)I_n(t-\tau)\,d\tau\right]\underline{\mathbf{e}}_n(\mathbf{r}). \tag{3}$$

By multiplying (3) by the test function $\underline{\mathbf{e}}_{n0}(x,y)$, integrating over the transverse waveguide cross section S, and considering the orthonormality properties of the $\underline{\mathbf{e}}_n(x,y)$, we obtain

$$\sum_{k,\mu,m,n} {}_ka_{\mu,m,n}T_k(t)\int_S\int \Phi_{\mu,m,n}(\mathbf{r})\underline{\mathbf{a}}_\mu\cdot\underline{\mathbf{e}}_{n0}(\mathbf{r})\,dS = \eta\left[I_{n0}(t) - \frac{\omega_{n0}}{2}\int_0^t J_1(\omega_{n0}\tau)I_{n0}(t-\tau)\,d\tau\right]. \tag{4a}$$

By following the same procedure used to find (4a), but subtracting (1b) from (1a) and testing with the function $\Phi_{\mu_0,m_0,n_0}(x,y)\underline{\mathbf{a}}_{\mu 0}$ instead of the function $\underline{\mathbf{e}}_{n0}(x,y)$, we get

$$\sum_k {}_kb_{\mu 0,m0,n0}T_k(t) = -\sum_n\omega_n\int_0^t J_1(\omega_n\tau)I_n(t-\tau)\,d\tau \cdot\frac{\eta}{2\Delta S}\int_S\int\Phi_{\mu 0,m0,n0}(\mathbf{r})\underline{\mathbf{a}}_{\mu 0}\cdot\underline{\mathbf{e}}_n(\mathbf{r})\,dS \tag{4b}$$

where, for the evaluation of the (4b), we considered $\Phi_{\mu,m,n}(\mathbf{r})$ as rectangular spatial orthogonal basis functions for which the following relation holds:

$$\int_S\int\Phi_{\mu 1,m1,n1}(\mathbf{r})\underline{\mathbf{a}}_{\mu 1}\cdot\Phi_{\mu 2,m2,n2}(\mathbf{r})\underline{\mathbf{a}}_{\mu 2}\,dS \cong \Delta S\delta_{\mu 1,\mu 2}\delta_{m1,m2}\delta_{n1,n2}$$

where ΔS represents the area of the elementary TLM cell, respectively, being $\delta_{p1,p2}$ unity for $p_1 = p_2$ and zero otherwise.

Finally, by multiplying both (4a) and (4b) by the Dirac impulse test function $\delta(t_0)$ (where $t_0 = k_0\Delta t$), integrating over the time variable, and considering that $T_k(t_0) = 0$ for $k \neq k_0$, we obtain

$$\sum_{\mu,m,n} {}_{k0}a_{\mu,m,n}T_{k0}(t_0)\int_S\int\Phi_{\mu,m,n}(x,y)\underline{\mathbf{a}}_\mu\cdot\underline{\mathbf{e}}_{n0}(\mathbf{r})\,dS = \eta\left[I_{n0}(t_0) - \frac{\omega_{n0}}{2}\int_0^{t_0} J_1(\omega_{n0}\tau)I_{n0}(t_0-\tau)\,d\tau\right] \tag{5a}$$

$${}_{k0}b_{\mu 0,m0,n0} = -\frac{\eta}{2\Delta S T_{k0}(t_0)}\sum_n\omega_n\int_0^{t_0} J_1(\omega_n\tau)I_n(t_0-\tau)\,d\tau \cdot\int_S\int\Phi_{\mu 0,m0,n0}(x,y)\underline{\mathbf{a}}_{\mu 0}\cdot\underline{\mathbf{e}}_n(x,y)\,dS. \tag{5b}$$

Note that $T_{k0}(t_0) = 1$.

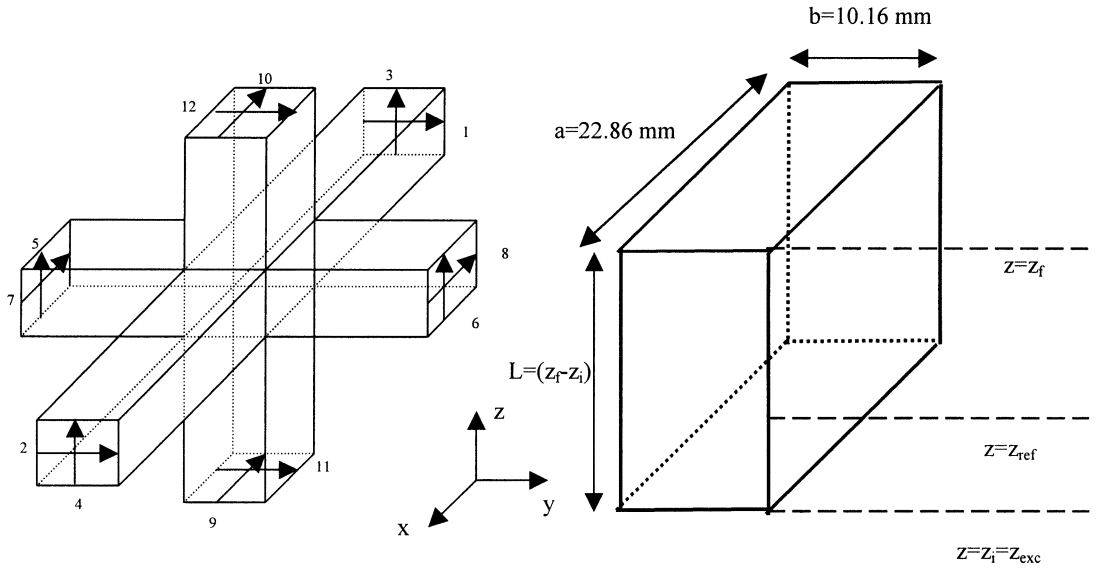

Fig. 2. Left-hand side: TLM node of the three-dimensional SCN. Right-hand side: analyzed rectangular waveguide (WR90) with $a = 22.86$ mm, $b = 10.16$ mm.

The time integral can be discretized using the TLM time step

$$\begin{aligned}\int_0^{t_0} & J_1(\omega_{n0}\tau) I_{n0}(t_0-\tau)\,d\tau \\ &\cong \sum_{k=0}^{k_0} J_1(\omega_{n0}k\Delta t) I_{n0}(t_0-k\Delta t)\Delta t \\ &= \sum_{k=1}^{k_0} J_1(\omega_{n0}k\Delta t) I_{n0}(t_0-k\Delta t)\Delta t.\end{aligned}$$

Note that the k-index starts from 1 because $J_1(0) = 0$ and no contribution to the integral arises from the unknown coefficient $I_{n0}(t_0)$. It arises from the already evaluated coefficients $I_{n0}(t)$ with $t < t_0$.

We rewrite (5a) and (5b) by using the discretized time-domain integral

$$\begin{aligned}I_{n0}(t_0) = {} & \frac{\omega_{n0}}{2}\sum_{k=1}^{k_0} J_1(\omega_{n0}k\Delta t) I_{n0}(t_0-k\Delta t)\Delta t \\ & + \frac{1}{\eta}\sum_{\mu,m,n} {}_{k0}a_{\mu,m,n}\int_S\int \Phi_{\mu,m,n}(x,y)\underline{\mathbf{a}}_\mu \\ & \cdot \underline{\mathbf{e}}_{n0}(\mathbf{r})\,dS \qquad (6a)\end{aligned}$$

$$\begin{aligned}{}_{k0}b_{\mu 0,m0,n0} = {} & -\frac{\eta}{2\Delta S}\sum_n \omega_n \sum_{k=1}^{k_0} J_1(\omega_n k\Delta t) I_n \\ & \times (t_0-k\Delta t)\Delta t \cdot \int_S\int \Phi_{\mu 0,m0,n0}(x,y)\underline{\mathbf{a}}_{\mu 0} \\ & \cdot \underline{\mathbf{e}}_n(x,y)\,dS. \qquad (6b)\end{aligned}$$

By using (6a), we are now able to evaluate the present value of the modal current $I_{n0}(t_0) = I_{n0}(k_0\Delta t)$ from the known past values of the modal currents $I_{n0}(t) = I_{n0}(k\Delta t)$ (being $k < k_0$) and from the present TLM-incident waves ${}_{k0}a_{\mu,m,n}$.

Finally, from (6b), we derive the present TLM-reflected wave from the known values $I_{n0}(k\Delta t)$ (being $k < k_0$).

An analogous procedure can be followed for the TM modes by using the modal admittances instead of the modal impedances

$$\begin{aligned}I_n(t) &= Y_n(t) * V_n(t) \\ &= \frac{1}{\eta}\left[V_n(t) - \omega_n\int_0^t J_1(\omega_n\tau)V_n(t-\tau)\,d\tau\right].\end{aligned}$$

Finally, after mathematical manipulations, as with the TE modes, the following formulas for the TM modes can be derived:

$$\begin{aligned}V_{n0}(t_0) = {} & \frac{\omega_{n0}}{2}\sum_{k=1}^{k_0} J_1(\omega_{n0}k\Delta t) V_{n0}(t_0-k\Delta t)\Delta t \\ & + \sum_{\mu,m,n} {}_{k0}a_{\mu,m,n}\int_S\int \Phi_{\mu,m,n}(x,y)\underline{\mathbf{a}}_\mu \\ & \cdot \underline{\mathbf{e}}_{n0}(\mathbf{r})\,dS \qquad (7a)\end{aligned}$$

$$\begin{aligned}{}_{k0}b_{\mu 0,m0,n0} = {} & \frac{1}{2\Delta S}\sum_n \omega_n \sum_{k=1}^{k_0} J_1(\omega_n k\Delta t) V_n(t_0-k\Delta t)\Delta t \\ & \cdot \int_S\int \Phi_{\mu 0,m0,n0}(x,y)\underline{\mathbf{a}}_{\mu 0}\cdot\underline{\mathbf{e}}_n(x,y)\,dS. \qquad (7b)\end{aligned}$$

III. Results

In order to test the method, we proceed to the following steps.

Step 1) Calculation of the residual reflection in a rectangular waveguide terminated by the MABCs, introduced by the present contribution.

Step 2) Calculation of the reflection coefficient in the same rectangular waveguide loaded by thick inductive irises.

A. Reflection Characteristics of the Absorbing Boundaries

We analyze a rectangular waveguide (WR90), shown in Fig. 2, with $a = 22.86$ mm, $b = 10.16$ mm, corresponding to a band of operation from 8 to 12 GHz for the TE_{10} mode.

The three-dimensional space of the structure is discretized by an SCN mesh, with the branches orientation shown in Fig. 2. We consider a Cartesian homogeneous mesh with $\Delta x = \Delta y = \Delta z = \Delta L = 0.381$ mm.

Our goal is to calculate the reflection coefficient of the empty rectangular guide with the absorbing boundaries generated by applying the MABC. We then compare the results with the reflection coefficient obtained by modeling the boundaries with: 1) the free-space boundary conditions: ${}_k a_{\mu,m,n} = 0$ [14] and 2) the diakoptics procedure [15].

In Fig. 2, we show the longitudinal section of the guide, with the position of: the left-hand-side ($z_i = 1$) and right-hand-side ($z_f = 800$) boundaries; the excitation plane ($z_{\rm exc} = 2$), being $z_p, (p = 1, \ldots, n)$ the discretization indexes along the z-direction. Considering the propagation in the TLM lattice, in order to distinguish and separate incident and reflected pulses, we consider a guide length $L = (z_f - z_i)\Delta L = 304.8$ mm (800 cells) and place the excitation point just at the left boundary. The wave-pulse traveling to the right-hand side is, after some time, reflected back by the right-hand-side absorbing boundary. Since the reference plane is placed at $z = z_{\rm ref} = 50$, we can distinguish between the incident and scattered fields. The excitation pulse is a sinusoidal electric field in the 8–12-GHz band, centered at $f = 10$ GHz, modulated by a Gaussian distribution and having the Ey-$\rm TE_{10}$ form as transversal spatial distribution. In order to excite such a modal configuration, we inject impulses into branch 11 (see Fig. 2) of all the nodes along the excitation planes, which is reported as follows:

$$ {}_k a_{11,m,n} = \sin\left(\frac{\pi}{a} x_m\right) \sin\left(\omega_0 (t_k - T_0)\right) \exp\left(-\frac{(t_k - T_0)^2}{\sigma}\right) \tag{8} $$

where $t_k = k\Delta t, (k = 1 \ldots n)$ is the k time step, $T_0 = 3\sigma^{1/2}$ is the time position where the Gaussian is centered, $\sigma = 12/(\pi(f_{\max} - f_{\min})$ being $f_{\max} = 12$ GHz and $f_{\max} = 8$ GHz, and $\omega_0 = 2\pi f_0$ with $f_0 = 10$ GHz. The time step is, according to the TLM algorithm, $\Delta t = \Delta L/2c = 0.635$ p/s, (c is the light velocity).

We consider $n = 5000$ time steps. The point x_m is the central point of the transverse cell indexes n and m. The resulting mesh size is $60 \times 30 \times 800$.

We now model the absorbing boundaries on the transverse planes placed in z_i and z_f by using the present method. In particular, the pulses of branches 11 of the nodes in the z_i-plane and of branch 12 of the nodes in the z_f-plane are generated by (6a) and (6b). Time separation between incident and reflected fields permits us to calculate the magnitude of reflection after fast Fourier transform (FFT).

In order to compare the above results, we now model the boundaries of the same waveguide by using the time-domain diakoptics technique [8], [9]. In time-domain diakoptics, the modeling of absorbing boundaries is performed by pre-simulating a semi-infinite waveguide and by using the time-domain impulse response (numerical Green's function) of such a structure in order to terminate the computational domain, as reported in [8] and [9].

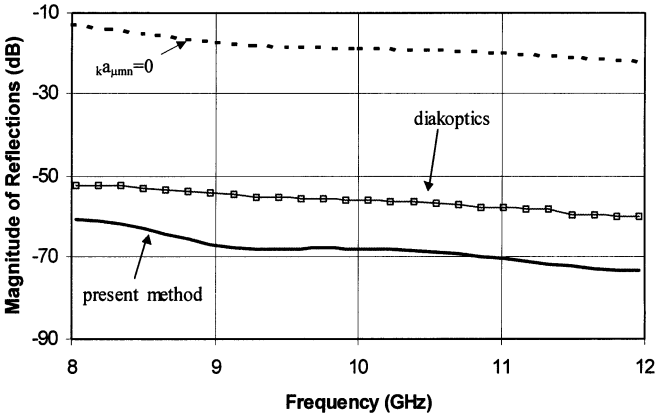

Fig. 3. Magnitude of the reflection coefficient calculated by applying the MABCs of the present method (continuous line) compared to the case of applying: diakoptics, [8], [9] (continuous line with squares) and ${}_k a_{\mu,m,n} = 0$ (dashed line).

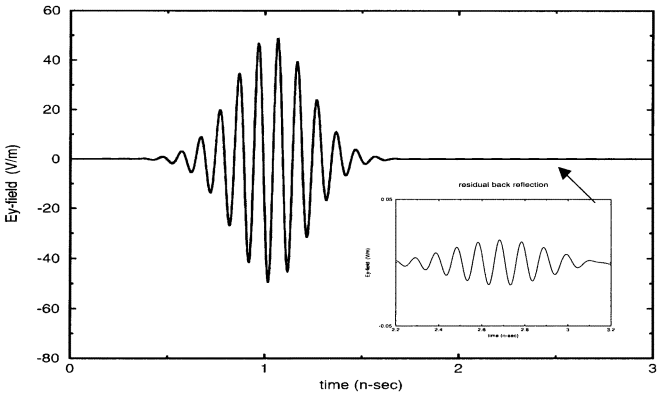

Fig. 4. Time behavior of the E_y-field at the center of the reference plane ($z_{\rm ref} = 50$) and the zoom of the residual back reflections. The field is referred to the MABC simulation of Fig. 3.

Another comparison is performed by applying the simplest closure of a TLM domain: the free-space boundary conditions ${}_k a_{11,m,n} = 0$ in z_i and ${}_k a_{12,m,n} = 0$ in z_f.

In Fig. 3, we report on the magnitude of the reflections. It is relevant to note that, by using the MABC method, only an extremely low level of field is back reflected; the overall magnitude of S_{11} is below 60 dB, thus confirming the validity of the approach. Time-domain diakoptics also provides very good results (8–10 dB above the MABC method), but it requires precomputation and storage of the time-domain impulse response.

In Fig. 4, we report on the time behavior of the E_y-field for the MABC simulation of Fig. 3 at the center of the cross section of the reference plane. Also in this figure, we insert the zoom of the very low residual back reflection (between 2–3 ns), which is not detectable in the normal proportion of this figure.

In such a configuration, only $\rm TE_{n0}$ modes are excited and the pulse values on branches 7–10 of the condensed node are always zero (because E_x and E_z are zero). Hence, we have nonzero pulse values only on the remaining eight branches.

We note that by using the free-space conditions (${}_k a_{\mu,m,n} = 0$), a noticeable level of field is back reflected. All the computations are performed with the same platform, i.e., 600-MHz PC,

TABLE I
COMPUTATIONAL TIME AND GRID PARAMETERS FOR THE CALCULATION OF THE REFLECTION CHARACTERISTICS OF ABSORBING BOUNDARIES IN THE EMPTY WR90 GUIDE OF FIGS. 2–4

$\Delta x=\Delta y=\Delta z=0.381$ mm $\Delta t=6.35$ psec	CPU – Time (minutes)	Mesh Size
MABC	22	60x30x600
Diakoptics	32	60x30x600
${}_{\kappa}a_{\mu,m,n}=0$	16	60x30x600

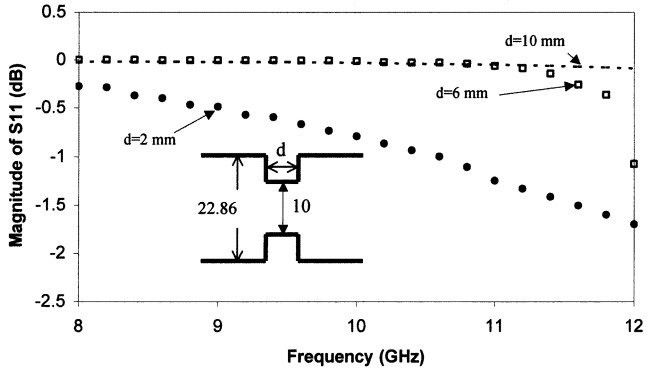

Fig. 5. Reflection-coefficient magnitude of the inductive iris in a WR90 waveguide depicted in the inset. The iris is of variable thickness d and the dimensions are expressed in millimeters.

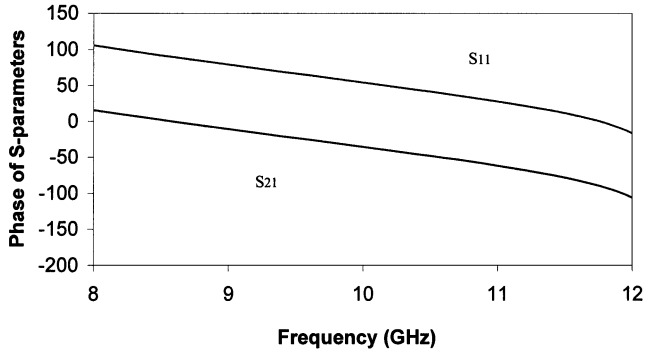

Fig. 6. As in Fig. 5, but for the phase of the scattering parameters in the case of $d = 6$ mm for the structure of Fig. 5. The reference planes in this case are placed 5 mm away from the iris.

500-MB RAM. In Table I, we show a comparison of computational times.

B. S-Parameters of a Thick Iris

We now introduce a thick iris of various thickness d inside the rectangular waveguide, as shown in the inset of Fig. 5. In this figure, we show the magnitude of S_{11} varying the d-parameter, while in Fig. 6, the phase of the scattering parameter for $d = 6$ mm are plotted. Finally, in Fig. 7, we show the magnitude of S_{12}, calculated by the present method and compared with the accurate solution by mode matching of [16], noting very good agreement.

The absorbing boundaries are generated by the MABC method by applying (6a)–(7b).

In order to compute the S-parameters of the discontinuity, we perform: 1) a computation without the discontinuity, providing the incident field and 2) a computation with discontinuity, providing the scattered and transmitted fields. In both cases, the corresponding pulses are nearly completely absorbed by the modeled boundaries. We could consider an arbitrary number of as modes, but 5–6 are sufficient, in the actual configuration, in order to absorb the energy of the excited higher order modes.

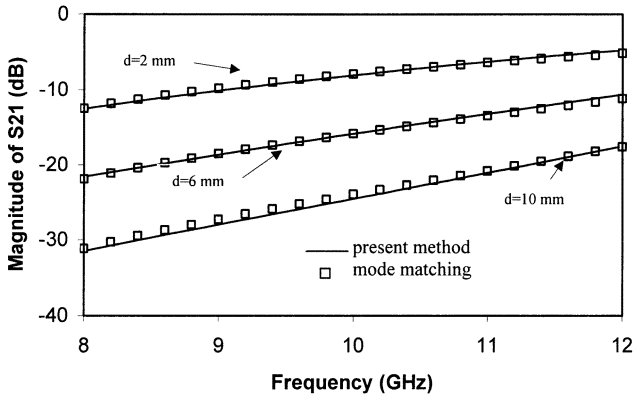

Fig. 7. As in Fig. 5, but for the transmission-coefficient magnitudes. In this figure, the comparison with the mode-matching method is reported [16].

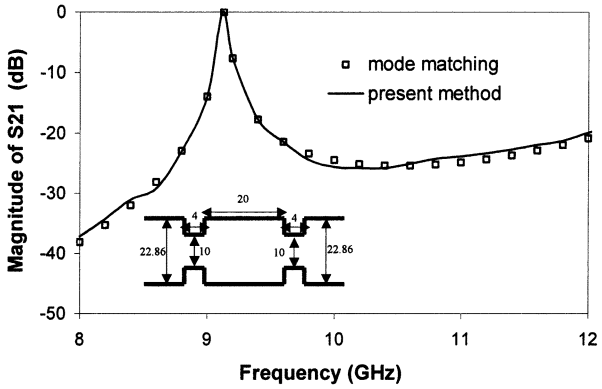

Fig. 8. Transmission coefficient for two cascaded inductive irises. The geometry of the structure is in the inset and the dimensions are in millimeters.

If we choose boundaries closer to the discontinuities, we reduce the three-dimensional (3-D) space to discretize, thus reducing memory effort and CPU time. However, in this case, a larger number of modes is necessary, thus providing an increased number of convolutions. The best compromise is to choose the absorbing boundaries a few cells away from the discontinuities and considering the first 4–5 modes.

C. S-Parameters of Two Cascaded Inductive Iris

As a cogent example, we now compute the S-parameters of two cascaded inductive irises.

In Fig. 8, the transmission parameter computed by the present method is compared with the results obtained by the mode-matching method in [16], showing a very good agreement. The geometry is inserted in this figure.

IV. CONCLUSION

In this paper, we have introduced exact TLM MABCs for closed homogeneous waveguides. This approach is based on applying to the TLM algorithm time-domain mode matching at the

boundaries, where the absorbing condition in the time domain is achieved by the convolution of the modal characteristic impedances, after the inverse Fourier transform.

The theory is developed for both TE and TM modes. The method is tested by computing the MABC reflection coefficient of the empty waveguide and then simulating: 1) a thick iris in a rectangular waveguide with variable size and 2) a cascade of two irises. The results obtained by the present MABC method are compared with those obtained by analytical methods in the literature, showing very good agreement and, thus, confirming a highly accurate wide-band match of the fundamental mode, as well as of higher order modes excited by the discontinuity.

REFERENCES

[1] P. B. Johns, "A symmetrical condensed node for the TLM method," *IEEE Trans. Microwave Theory Tech.*, vol. MTT-35, pp. 370–377, Apr. 1987.

[2] K. S. Yee, "Numerical solution of initial boundary value problems involving Maxwell's equations in isotropic media," *IEEE Trans. Antennas Propagat.*, vol. AP-14, pp. 302–307, May 1966.

[3] Z. Chen, M. M. Ney, and W. J. R. Hoefer, "Absorbing and connecting boundary conditions for the TLM method," *IEEE Trans. Microwave Theory Tech.*, vol. 41, pp. 2016–2024, Nov. 1993.

[4] C. Eswarappa and W. J. R. Hoefer, "One-way equation absorbing boundary conditions for 3-D TLM analysis of planar and quasi-planar structures," *IEEE Trans. Microwave Theory Tech.*, vol. 42, pp. 1669–1677, Sept. 1994.

[5] N. Kukutsu and R. Konno, "Super absorption boundary condition for guided waves in the 3-D TLM simulation," *IEEE Microwave Guided Wave Lett.*, vol. 5, pp. 299–301, Sept. 1995.

[6] J. P. Bèrenger, "A perfectly matched layer for the absorption of electromagnetic waves," *J. Comput. Phys.*, vol. 114, no. 2, pp. 110–117, Oct. 1994.

[7] C. Eswarappa and W. J. R. Hoefer, "Implementation of Bèrenger's absorbing boundary conditions in TLM by interfacing FDTD perfectly matched layers," *Electron. Lett.*, vol. 31, no. 15, pp. 1264–1266, July 1995.

[8] M. Righi and W. J. R. Hoefer, "Efficient 3-D SCN–TLM diakoptics for waveguide components," *IEEE Trans. Microwave Theory Tech.*, vol. 42, pp. 2381–2385, Dec. 1994.

[9] ——, "Efficient hybrid TLM/mode matching analysis of packaged components," in *IEEE MTT-S Int. Microwave Symp. Dig.*, vol. 42, Dec. 1996, pp. 447–450.

[10] F. Moglie, T. Rozzi, P. Marcozzi, and A. Schiavoni, "A new termination for the application of FDTD techniques to discontinuity problems in close homogeneous waveguide," *IEEE Microwave Guided Wave Lett.*, vol. 2, pp. 475–477, Dec. 1992.

[11] F. Moglie, T. Rozzi, and P. Marcozzi, "Wide-band matching of waveguide discontinuities by FDTD methods," *IEEE Trans. Microwave Theory Tech.*, vol. 42, pp. 2093–2098, Nov. 1994.

[12] F. Alimenti, P. Mezzanotte, L. Roselli, and R. Sorrentino, "Modal absorption in the FDTD method: A critical review," *Int. J. Numer. Modeling*, vol. 10, pp. 245–264, May 1997.

[13] A. Kreczkowsky, T. Rutkowsky, and M. Mrozowsky, "Fast modal ABC's in the hybrid PEE–FDTD analysis of waveguide discontinuities," *IEEE Microwave Guided Wave Lett.*, vol. 9, pp. 186–188, May 1999.

[14] T. Itoh, *Numerical Techniques for Microwave and Millimeter-Wave Passive Structures*. New York: Wiley, 1989, pp. 496–591.

[15] J. Uher, S. Liang, and W. J. R. Hoefer, "S-parameter of microwave components computed with the 3D-condensed symmetrical TLM node," in *IEEE MTT-S Int. Microwave Symp. Dig.*, vol. 2, pp. 653–656.

[16] A. Weisshaar, M. Mongiardo, A. Tripathi, and K. Tripathi, "CAD-oriented full-wave equivalent circuit models for waveguide components and circuits," *IEEE Trans. Microwave Theory Tech.*, vol. 44, pp. 2564–2570, Dec. 1996.

Luca Pierantoni (M'94) was born in Moie di Maiolati Spontini, Italy, in 1962. He received the Laurea degree (*summa cum laude*) in electronics engineering and Ph.D. degree in electronics and automatics from the University of Ancona, Ancona, Italy, in 1988 and 1993, respectively.

From 1990 to 1995, he was a Research Fellow with the Department of Electronics and Automatics, University of Ancona. From 1996 to 1999, he was a Senior Research Scientist with the Institute of High-Frequency Engineering, Technical University of Munich, Munich, Germany, where he was involved with a research project supported by the Deutsche Forschungsgemeinschaft. Since February 1999, he has been the Department of Electronics and Automatics, University of Ancona, where he is currently an Assistant Professor. His current research interests are in the development and applications of analytical–numerical methods for the analysis of microwave circuits and radiation problems.

Cristiano Tomassoni was born in Spoleto, Italy, in 1969. He received the Laurea degree and Ph.D. degree in electronics engineering from the University of Perugia, Perugia, Italy, in 1996 and 1999, respectively.

In 1999, he was a Visiting Scientist with the Lehrstuhl für Hochfrequenztechnik, Technical University of Munich, Munich, Germany. In 2001 he was a Guest Scientist with the Fakultät für Elektrotechnik und Informationstechnik, Otto-von-Guericke University, Magdeburg, Germany. He is currently a Research Fellow with the University of Perugia. His main area of research is the modeling of waveguide discontinuities. His research interests also include the development of hybrid methods for the design of microwave components and for the modeling of electromagnetic compatibility (EMC) problems.

Tullio Rozzi (M'66–SM–74–F'90) received the Dottore degree in physics from the University of Pisa, Pisa, Italy, in 1965, the Ph.D. degree in electronic engineering from the University of Leeds, Leeds, U.K., in 1968, and the D.Sc. degree from the University of Bath, Bath, U.K., in 1987.

From 1968 to 1978, he was a Research Scientist with Philips Research Laboratories, Eindhoven, The Netherlands. In 1975, he spent one year with the Antenna Laboratory, University of Illinois at Urbana-Champaign. In 1978, he was the Chair of Electrical Engineering at the University of Liverpool. In 1981, he was the Chair of Electronics and Head of the Electronics Group at the University of Bath, where he was also Head of the School of Electrical Engineering on an alternate three-year basis. Since 1988, he has been a Professor and is currently Head of the Department of Electronics and Automatics, University of Ancona, Ancona, Italy.

Dr. Rozzi was the recipient of the 1975 IEEE Microwave Theory and Technique Society (IEEE MTT-S) Microwave Prize.